JOURNAL OF ENGINEERING RESEARCH

Refereed and issued twice annually by the
Faculty of Engineering - University of Tripoli

Issue 28 September 2019

NUMERICAL STUDY OF LOW LAMINAR FLOW IN A PIPE WITH A SUDDEN EXPANSION USING FINITE VOLUME TECHNIQUE

Tuhami M. Jaballa and Mohammed K. Yosef

Department of mechanical Engineering. University of Tripoli- Libya
E-mail: t.jaballa@out.edu.ly mkzmlf@yahoo.com

الملخص

يقدم البحث دراسة عددية مفصلة للتدفق الطبقي المنخفض في أنبوب به توسع مفاجئ في منطقة المقطع العرضي. أعتبر التدفق محوري متماثل ومستقرة. شملت الدراسة الحل العددي لمعادلات نافير– ستوكس باستخدام طريقة الحجم المحدود. كذلك تم استخدام برنامج حاسوبي قائم على خوارزمية (SIMPLE) لبناء نموذج رياضي من أجل حل نظام معادلات الاستمرارية ومعدل كمية الحركة. أثبتت الدراسة أن الحل العددي المقترح كان قادراً على حساب اختلافات السرعة المحورية في اتجاه نصف القطر, والسرعة المركزية وميزات التدفق المختلفة مثل (منطقة إعادة التدوير وطول إعادة الارتباط وطول إعادة التطور). واستخدم برنامج حاسوبي بلغة (FORTRAN 90) لتنفيذ الحل العددي. تم فحص المشكلة لقيم مختلفة لأعداد رينولدز في المدى المنخفض من 20 إلى 600 ونسبة توسع ثابتة هي (ER=2). أظهرت النتائج العلاقة بين طول إعادة الارتباط وطول إعادة التطور بأرقام رينولدز المختلفة, وقد وجد أن طول إعادة الارتباط وطول إعادة التطور كان دالة خطية مع رقم رينولدز. تم مقارنة نتائج نموذج إعادة الإرتباط مع عدد رينولدز في المدى من 20.6 إلى 211 مع النتائج التجريبية المتاحة للتحقق من صحة النموذج الحسابي المستعمل.

ABSTRACT

The research presents a detailed numerical study of low laminar flow in a pipe with a sudden expansion in its cross sectional area. The flow considered to be steady and axi-symmetric. The study involved a numerical solution of the Navier-Stokes equations by using finite volume method. A computational code based on the algorithm SIMPLE was used to formulate a mathematical model to solve the mass and momentum equations. The prepared numerical solution was capable of calculating the axial velocity, the centerline velocity and the different flow features such as (recirculation zone, reattachment length and redevelopment length).

A computer program in (FORTRAN 90) was used to carry out the numerical solution. The problem was examined for different values of Reynolds numbers in the range from 20 to 600 and fixed expansion ratio is (ER=2). The results show the relationship between the reattachment length and redevelopment length with different Reynolds numbers. It was found that the reattachment length and the redevelopment length was a linear function of the Reynolds number. The results of the reattachment length with Reynolds number in the range from 20.6 to 210 are compared with available experimental results to validate the present computational model.

KEYWORDS: Low Re Laminar Flow; Sudden Expansion in a Pipe; Axial Velocity Profile; Recirculation Zone; Reattachment Length; Redevelopment length.

INTRODUCTION

On the pipelines, some elbows, tees and reducer joints are installed for controlling and regulating flow in the pipe. While the flowing fluid through those accessories the uniform flow will be disturbed in the local area due to change of wall or flow rate, leading to change of value direction or distribution of flow speed. Due to the inertia when fluid flows from a pipe with a smaller diameter to pipe with bigger diameter, the flow will be expanded gradually rather than suddenly. Whirlpool will be formed between the corner of the pipe and mainstream and rotates with the main stream, the rotation process will consume energy and flow impact, and collision caused by the sudden change of the pipe section will bring losses of the mechanical energy. The importance of flow through sudden changes in flow passages found in the numerous industrial applications. In this particular case the pipe experiences a sudden expansion with a ratio of the outlet diameter to the inlet diameter of 2 (D/d=2) resulting in a variety of interesting flow features. At the entrance, the flow has a fully developed velocity profile. At the expansion the flow undergoes separation that in turn produces a recirculation zone. After what is known as the reattachment length, (X_r), the flow reattaches and there is no more recirculation. The flow achieves a fully developed profile for the new diameter after the redevelopment length, (L_d). A two-dimensional computational domain has been chosen for analysis considering the steady state.

The effects of flow rates are investigated with constant diameter ratio to understand the flow characteristics for sudden expansion. The size of the recirculation zone, flow reattachment length, redevelopment of flow and recirculating flow strength depends on several parameters, primarily on flow rate i.e. Reynolds number, expansion ratio and flow direction.

LITERATURE REVIEW

Macagno and Hung1967 [1] carried out an experimental study and numerically study in the sudden expansion configuration in axi-symmetric flow for a Reynolds number ranging from 36 to 4500, by means of computational simulation, for ER= 2 and of Reynolds number up to 200. They concluded that, for laminar flow, the main role of eddy is that of shaping the flow with rather a small energy exchange.

Durst et al. 1993 [3] studied the symmetric sudden expansion flow at low Reynolds numbers and ER=2. Experimental and numerical predictions, confirmed short separation zone for Reynolds numbers above 125, they observed the increase in length of the long separation region while the short remains approximately constant as the Reynolds number increased above 125. They used laser-Doppler anemometer (LVA) to obtain the experimental data. Numerical predictions were made using finite volume method.

Oliveira and Pinho1997 [4] carried out a numerical study of laminar flow of a Newtonian fluid in an axi-symmetric pipe expansion in Reynolds number $\leq$ 225 and ER=2.6. They adopted a finite-volume approach for the computational work. The results obtained from the numerical work for the overall flow characteristics, such as recirculation length, its strength, and center location, were compared with available experimental data and correlations, and good agreement was obtained. The main motivation of this investigation was to evaluate the pressure-loss coefficient for a range of Reynolds numbers <225 and compared the results with existing simplified theory, they observed that pressure increasing as the fluid decelerates thus creating a recirculation zone and the pressure variation attributable to fully developed friction on the wall.

Hammad et al. 1999 [5] Used real-time digital particle image velocimetry (PIV) for an experimental study of the laminar flow through an axis-symmetric sudden expansion with an expansion ratio 2. In their experiment the measurements covered the regions of separation, reattachment and re-development. Two dimensional velocity maps were obtained on the vertical center plane for six Reynolds numbers between 20 and 211. They studied the dependence of reattachment length, redevelopment length and recirculating flow strength of the Reynolds number. They observed that not only the reattachment length, but also the redevelopment length downstream of reattachment was a linear function of the Reynolds number, while the recirculation eddy strength, on the other hand, was dependent nonlinearly on the Reynolds number. They also observed that recirculation eddy strength became weaker as the Reynolds number increased.

Ray and Prokash, 2012 [6] carried out a numerical study of laminar flow in a sudden expansion pipe with an expansion ratio ER=2, 4 and 8, the flow separation and flow reattachment phenomena occurs in the concave wall in the downstream of sudden expansion geometry for Re=20 and ER=4. For Re=200, ER=4, flow asymmetry is clearly observed; as the size and length of the flow vortices (on both walls), this phenomena suggests that the flow has already entered the unstable regime, and also that the instability is more in the flow with higher expansion ratio (ER). It is observed that at ER=4 and Re=300, the length of the flow reattachment point at left wall increases and at right wall decreases. Also, there is a formation of the weaker secondary vortex, the size of this secondary vortex increases with increase in ER for the same Reynolds number, it is observed that the flow reattachment length increases linearly with increase in Re for fixed ER, it is seen that in the case of ER=2, there is no asymmetry, for the cases of Er=4 and 8, this instability is clearly visible above a particular value of Re. At Re=223, the velocity decreases slightly after the point of sudden expansion with an increase in Xr and there is a smaller variation in velocity with the increase in ER, pressure in decreases with increase in Xr and reaches a minimum value at the point of sudden expansion and again P increases with increase in Xr and there is a smaller variation in P with the increase in ER.

Veronica M, Petrio 2014 [7] carried out a numerical study of laminar flow in sudden expansion configuration, they observed, after the expansion the flow has a decrease in the velocity and a recirculation zone develops. Considering the result of the numerical simulation of the three meshes the relation between the reattachment length and the Reynolds number follows a linear profile. Considering the different grid size used the error in some cases increases and in other cases decreases.

Li Yinpeng and Wang. 2015 [8] They carried out an experimental study to measure value of the local resistance coefficient of sudden expansion pipe, 3.126, significantly different from the theoretical value 2.434. Error of local head loss is only 22%. They observed, for sudden expansion pipe, the increment of the flow-carrying section will lead to the decrement of average velocity and velocity head of flow. Therefore, in the designing of pipeline, local resistance coefficient of the sudden expansion pipe measured through experiment is more close to the actual value.

MATHEMATICAL MODEL

The governing equations

Predictions of the laminar flow field in a sudden pipe expansion were obtained numerically by solving the governing two-dimensional elliptic partial differential equations, the flow was considered to be axi-symmetric as in Figure (1). The flow field can often be solved by

considering mass conservation and momentum equations only. The energy equation needs to be solved only if the problem involves heat transfer.

Continuity equation

The general equation of continuity in two-dimensional and cylindrical coordinate flow is expressed as follows:

$$\frac{\partial \rho}{\partial t} + \frac{1}{r}\frac{\partial}{\partial x}(r\,\rho\,U) + \frac{1}{r}\frac{\partial}{\partial r}(r\,\rho\,V) = 0 \quad (1)$$

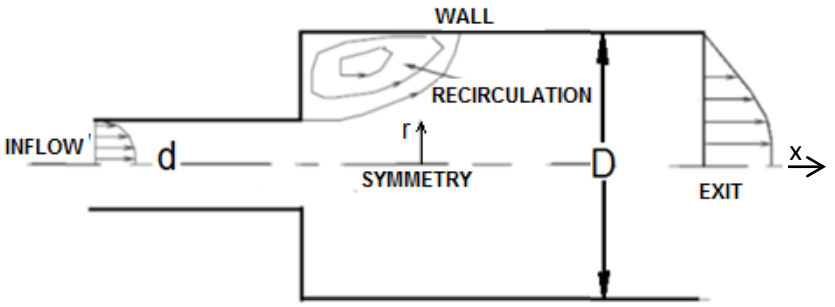

Figure 1: Sudden expansion configuration [1].

Where U and V are the velocity component. For a compressible steady state conditions the equation of continuity becomes:

$$\frac{1}{r}\frac{\partial}{\partial x}(r\;\rho\,U) + \frac{1}{r}\frac{\partial}{\partial r}(r\,\rho\,V) = 0 \quad (2)$$

The equation of motion

To develop the equation of motion, we start from the Newton law of conservation of energy.

((Rate of momentum accumulation = transport rate of momentum in - transport rate of momentum out + sum of forces acting on the element)). The result is:

x -Momentum equation:

$$\frac{\partial \rho\, U}{\partial t} + \frac{1}{r}\left[\frac{\partial}{\partial x}(r\,\rho\,UU)\right] + \frac{1}{r}\left[\frac{\partial}{\partial r}(r\,\rho\,UV)\right] = -\frac{\partial P}{\partial x} + \frac{1}{r}\frac{\partial}{\partial \mathrm{x}}\left[r\,\mu\,\frac{\partial U}{\partial x}\right] + \frac{1}{r}\frac{\partial}{\partial \mathrm{r}}\left[r\,\mu\,\frac{\partial U}{\partial r}\right] + S_U \quad (3)$$

r -Momentum equation:

$$\frac{\partial \rho\, V}{\partial t} + \frac{1}{r}\left[\frac{\partial}{\partial x}(r\,\rho\,UV)\right] + \frac{1}{r}\left[\frac{\partial}{\partial r}(r\,\rho\,VV)\right] = -\frac{\partial P}{\partial r} + \frac{1}{r}\frac{\partial}{\partial \mathrm{x}}\left[r\,\mu\,\frac{\partial V}{\partial x}\right] + \frac{1}{r}\frac{\partial}{\partial \mathrm{r}}\left[r\,\mu\,\frac{\partial V}{\partial r}\right] + s_V \quad (4)$$

Where S_U, S_V Are source term, the source term included all terms which not important in the equation.

There are significant commonalities between the various equations. If we introduce a general variable ∅ the conservative form of all fluid flow equations, including equations for scalar quantities such as temperature and pollutant concentration etc., can usefully be written in the following form:

$$\frac{\partial \rho \phi}{\partial t} + \frac{\partial}{r\partial x}\left(r\rho U\phi\right) + \frac{\partial}{r\partial r}\left(r\rho V\phi\right) = -\frac{\partial p}{\partial x} + \frac{\partial}{r\partial x}\left[r\cdot\Gamma\frac{\partial \phi}{\partial x}\right] + \frac{\partial}{r\partial x}\left[r\cdot\Gamma\frac{\partial \phi}{\partial r}\right] + S_o \quad (5)$$

Unsteady Term | Convection term | Pressure term | Diffusion term | Source term

THE FINITE VOLUME FORMULATION:

The finite volume method is based on three steps:

1. Dividing the solution domain into discrete control volumes (Figure 2).
2. Integration of the governing equations over control volumes to yield a discretized equations.
3. Discretized equations must be set up at each of the nodal Points in order to solve the problem, the result set of algebraic equations is solved by using an iterative method. Thomas algorithm or the tri-diagonal matrix algorithm (TDMA).

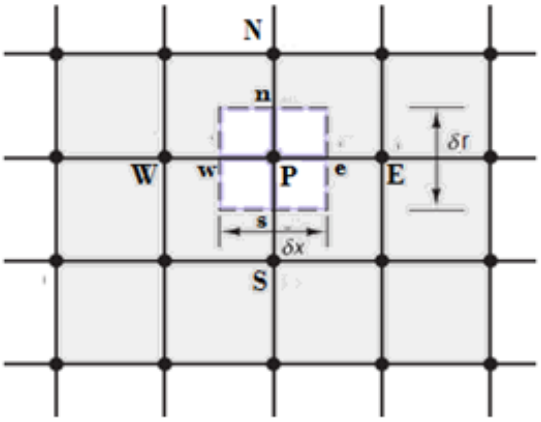

Figure 2: control Volume

DISCRETIZATION OF GOVERNING EQUATIONS

The purpose of any DISCRETIZATION practice is to transform the partial differential equations into a corresponding system, algebraic equations by the integration of the governing equation over a control volume to yield a discretized equation at its nodal point *P.*

Discretization of continuity

$$(\rho U A)_e - (\rho U A)_w + (\rho VA)_n - (\rho V A)_s = 0 \quad (7)$$

$$C_e - C_w + C_n - C_s = 0 \quad (8)$$

Discretization of the general transport equation

$$C_e\emptyset_P - C_w \emptyset_W + C_n\emptyset_P - C_s\emptyset_S =$$

$$D_e(\emptyset_E - \emptyset_P) - D_w(\emptyset_P - \emptyset_W) + D_n(\emptyset_N - \emptyset_P) - D_s(\emptyset_P - \emptyset_S) + S_P \emptyset_P + S_\emptyset \quad (9)$$

The discretization form can be rearranged as:

$$(C_e + C_n + D_e + D_w + D_n - D_s - S_P)\emptyset_P =$$

$$(C_w - D_w)\emptyset_W + (D_e)\emptyset_E + (C_s - D_s)\emptyset_s + (D_n)\emptyset_N + S_U \quad (10)$$

The coefficients of the property $\emptyset$ are defined as:

$$a_P = (C_e + C_n + D_e + D_w + D_n - D_s - S_P) \quad (11)$$

$$a_W = (C_w - D_w) \quad (12)$$

$$a_E = (D_E) \quad (13)$$

$$a_S = (C_S - D_S) \quad (14)$$

$$a_N = (D_N) \quad (15)$$

Let the source term be: $S_U = b$

By Substituting the above equations in the general discretization form, we can obtain The final form of the Discretized transport equations.

$$a_P \ \emptyset_P = a_W \ \emptyset_W \ + \ a_E \emptyset_E \ + \ a_S \emptyset_S \ + \ a_N \emptyset_N \ + b \quad (16)$$

There are many discretization methods for calculation of the value of transporting properties $\emptyset_e, \emptyset_w, \emptyset_n$ and $\emptyset_s$ on the control volume face.

1. The Upwind differencing scheme.
2. The hybrid differencing scheme.
3. Central differencing scheme.
4. The power-low scheme.
5. QUICK scheme.
6. TVD scheme.

The upwind differencing scheme, the central differencing scheme and hybrid differencing scheme are used for calculation of the value of transport property $\emptyset$ at the control volume faces. The central differencing scheme is employed in small Peclet numbers (Pe $<$ 2) and the upwind scheme is employed in large Peclet numbers (Pe $\geq$ 2). **Peclet number** is a measure of the relative strengths of convection and diffusion $P_e = \frac{\rho U}{\mu/\delta x}$ see Table (1).

Table 1: The representation of the convective, diffusive and Peclet number.

Peclet number	The contribution C
$\lvert P_e \rvert < 2$	$(\rho U)_w A_w(\emptyset_W + \emptyset_P)/2 - (\Gamma)_w A_w(\emptyset_P - \emptyset_W)/\delta x$
$P_e \geq 2$	$(\rho U)_w A_w \emptyset_W$
$P_e \leq -2$	$(\rho U)_w A_w \emptyset_P$

THE STAGGERED GRID

Grids are generated by using algebraic functions for grid spacing (non-uniform or uniform grid spacing). The staggered grid points are first developed. They are represented as i and j for x and r directions, respectively. The main grid points are calculated by using the staggered grid locations. Figure (3) shows the staggered and main grid locations. i and I, respectively in the x

direction on a ni x nj domain or (22x22) grid. The staggered grid starts with i=2 whereas the main grid starts with I=1. Note that the point (i=2) is the same as the point (I=1), and that ni=NI.

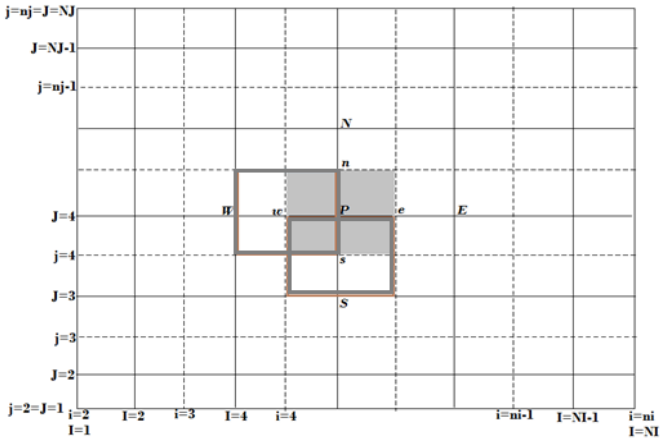

Figure 3: Main and Staggered grid location.

Boundary conditions:

• Inlet $U_{in} = U_{max}(r/R)^{**}2$ (17)

• Outlet $\frac{\partial U}{\partial x} = \frac{\partial V}{\partial x} = 0$ (18)

• Wall U = V = 0 (19)

Symmetry $\frac{\partial U}{\partial r} = 0 \ , V = 0$ (at r = 0) (20)

The solution procedure

1. A finite volume procedure is used in which the dependent variables are the velocity components and pressure.
2. The pressure is deducted from an equation which is obtained from the coupled continuity and momentum equations (yielding the Poisson equation for pressure).
3. At each iteration, the program calculates a first approximation of *u, v*, and *p* followed by a succeeding correction.
4. The procedure incorporates displaced grids for the axial and radial velocities *u* and *v*, which are placed between the nodes where the pressure *p* is stored.
5. An implicit line-by-line relaxation technique is employed in the solution procedure (requiring a tridiagonal matrix to be inverted in order to update a variable at all points along a column), using the TDMA (tri-diagonal matrix algorithm).

THE Semi-Implicit Methods for Pressure Linked Equations (SIMPLE) ALGORITHM:

The algorithm was originally put forward by Patankaer 1972, and is essentially a guess-and-correct procedure for the calculation of pressure on the staggered grid arrangement. The method is illustrated by considering the two-dimensional laminar steady flow equations. To initiate the SIMPLE calculation process a pressure field P^* is guessed. Discredited momentum equations are solved using the guessed pressure field to yield velocity components u^* and v^* as follows:

The velocity u at western face, for example:

$$u_w = d_w\,(P_W - P_P) \tag{21}$$

$$u'_w = d_w(P'_W - P'_P) \tag{22}$$

$$u = u^* + u' \tag{23}$$

$$u_w = u^* + d_w(P'_w - P'_P) \tag{24}$$

The general equation for the pressure correction P' is given by:

$$a_{I,J}P'_{I,J} = a_{I+1,J}P'_{I+!,J} + a_{I-1,J}P'_{I-1,J} + a_{I,J+1,}P'_{I,J+1} + a_{I,J-1}P'_{I,J-1} + b'_{I,J} \tag{25}$$

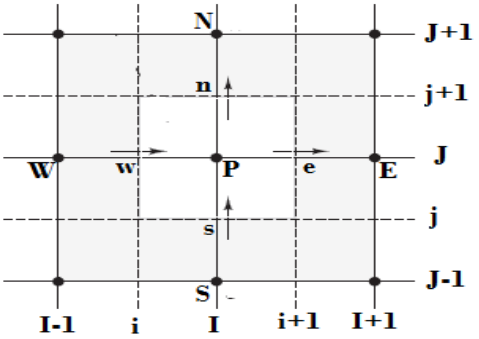

Figure 4: The scalar control volume used for discretisation of the continuity equation.

THE TDMA SOLVER

This process results in a system of linear algebraic equations which needs to be solved. The TDMA is applied along north–south (*n–s*), lines. The discretized equation is rearranged in the form:

$$-a_S\,\emptyset_S + a_P\,\emptyset_P - a_N\,\emptyset_N = a_W\,\emptyset_W + a_E\,\emptyset_E + b_P \tag{26}$$

Let

$$G_j = a_W\,\emptyset_W + a_E\,\emptyset_E + b_P \tag{27}$$

$$\alpha_j = a_N \tag{28}$$

$$\beta_j = a_S \tag{29}$$

$$K_j = a_P \tag{31}$$

Inserting these variables into equation (26) we get:

$$-\beta_j\,\emptyset_S + K_j\,\emptyset_P - \alpha_j\,\emptyset_N = G_j \tag{32}$$

This equation can now be solved along the north - south direction for values j=2 to n.

RESULTS AND DISCUSSION

Grid Independency Study

The uniform orthogonal finite-volume grid was mapped to the computational domain. The cells are non-uniformly spaced in the (x) direction and in the cross-stream (r) direction in order to place a higher number of cells near the sudden expansion region and near the no-slip walls where the flow experiences large spatial gradient. A grid refinement study was performed at an expansion ratio (*ER* = 2) by varying the number of

cells. Meshes of 13x13, 16x16, 19x19, 22x22 and 23x23 were used. The results of the grid independenc analysis are presented in table (2), by using the reattachment length with a fixed Reynolds number= 210. It is observed that the grid (22x22) is sufficient to ensure a grid independent solution, any, increase in the size of the grid shows no significant change in reattachment length with different grid sizes at the fixed Reynolds number, as described in Table (2).

Table 2: Grid independence study at Re = 210.

Grid size	Reattachment length (Xr/D)	Variation %
13x13	3	---
16x16	5.5	45%
19x19	8.4	34%
22x22	8.8	4.5%
23x23	8.8	0.00%

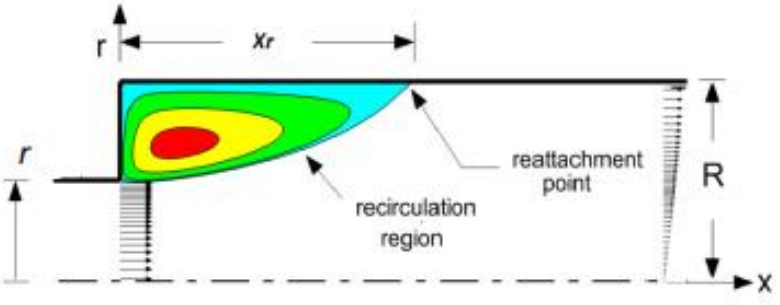

Figure 5: Separation region and reattachment point.

In Figure (6) and Figure (7), at grid (22x22) we observed that the reattachment length and the re-development length increase with increase in Reynolds number for fixed expansion ratio.

Reynolds number *Re*	Reattachment length Xr/D
20.6	1.1
55.4	2.6
77.6	3.8
100	4.6
156	7.1
210	8.8
225	9.2
300	12.7
350	13.3
400	16.1
450	16.7
600	22.1

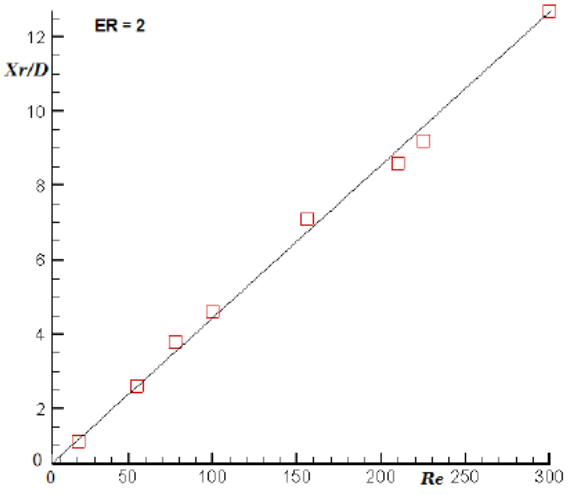

Figure 6: Reattachment length with range Reynolds number $20.6 \leq Re \leq 600$ For grid 22x22.

Reynolds Number *Re*	Redevelopment Length Le/D
20.6	1.236
55.4	3.324
77.6	4.656
100	6.1
56	9.36
210	12.6
225	13.5
300	18
350	21
400	24
450	27
600	36

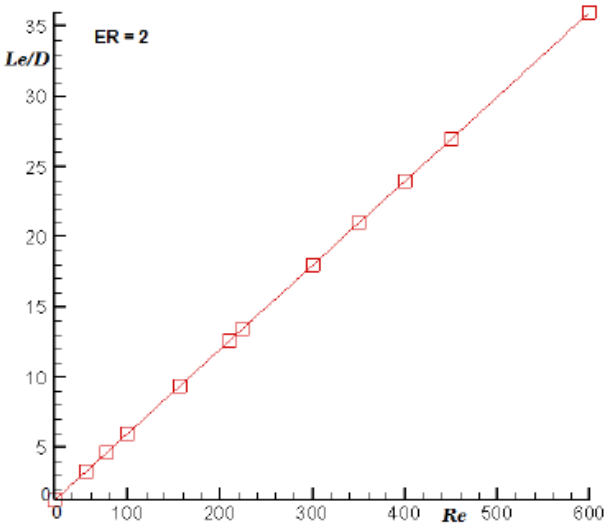

Figure 7: Redevelopment length with range Reynolds number $20.6 \leq Re \leq 600$ for grid 22x22.

CODE VALIDATION

The present numerical solution is verified by comparing present results with experimental study for Hammad, 1999 [5] and Macagno and Hung1967 [1], at low Renolds number from Re=20.6 to Re=210. As shown in Figure (8), the present work predictions are very close to the experimental published work results.

Reynolds Number *Re*	Redevelopment Length Le/D
20.6	1.236
55.4	3.324
77.6	4.656
100	6.1
56	9.36
210	12.6
225	13.5
300	18
350	21
400	24
450	27
600	36

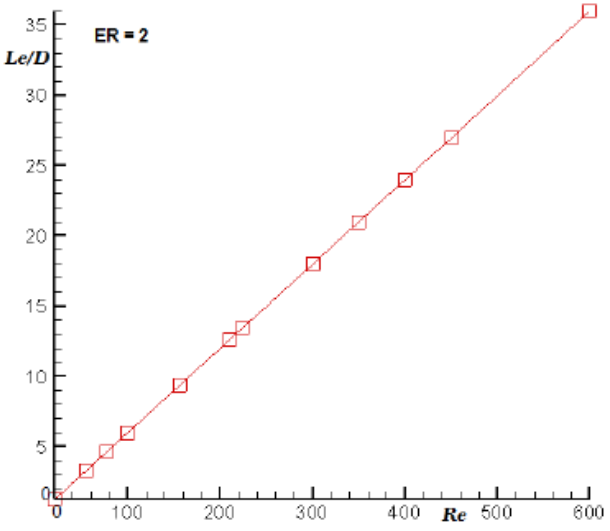

Figure 8: Comparison of the reattachment length at different Reynolds number with Hammed [5], and Macagno & Hung [1].

The relationship between the reattachment length and the Reynolds number is seen to be linear when Re is low. Considering the real-time digital particle image velocimetry (PIV) as a reference, the error in the predicted values is given in figure (8). It can be seen that the greatest variation is 11.3% at Re=77.6 , and the smallest is 3.8% at Re=55.4.

DESCRIPTION OF THE REVERSED FLOW VELOCITY

The predicted velocity is found to have two main regions; The first region is the shear layer separation and reattachment downstream of the sudden expansion, The second is the recirculation region. velocity and streamlines are described on contour plots. The flow recirculation occurs in the low-momentum fluid near the wall in response to the local adverse pressure gradient. Figures (9, 10 and 11) show the velocity profile from the $Re =$ 100, 300 and 400 for ER = 2 cases.

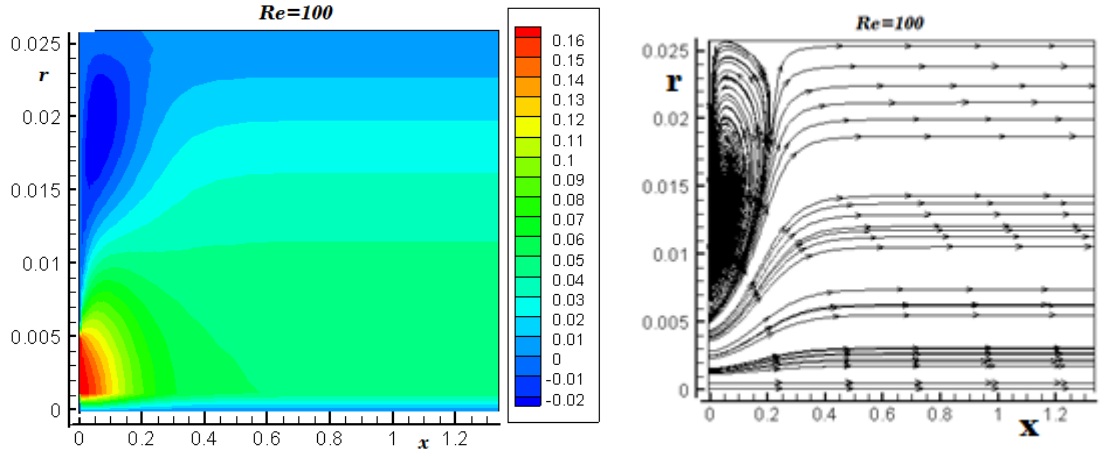

Figure 9: Contour plots of velocity U and Streamline in the recirculation zone for Re =100

The parabolic laminar velocity profile upstream of the expansion is altered downstream and a reversed-flow velocity profile developments in the near-wall regions on both sides. As the flow travels farther downstream of the expansion, the magnitude of the reverse velocity initially increases in response to the adverse pressure gradient and then decreases until the reversed flow disappears at the point of shear layer reattachment.

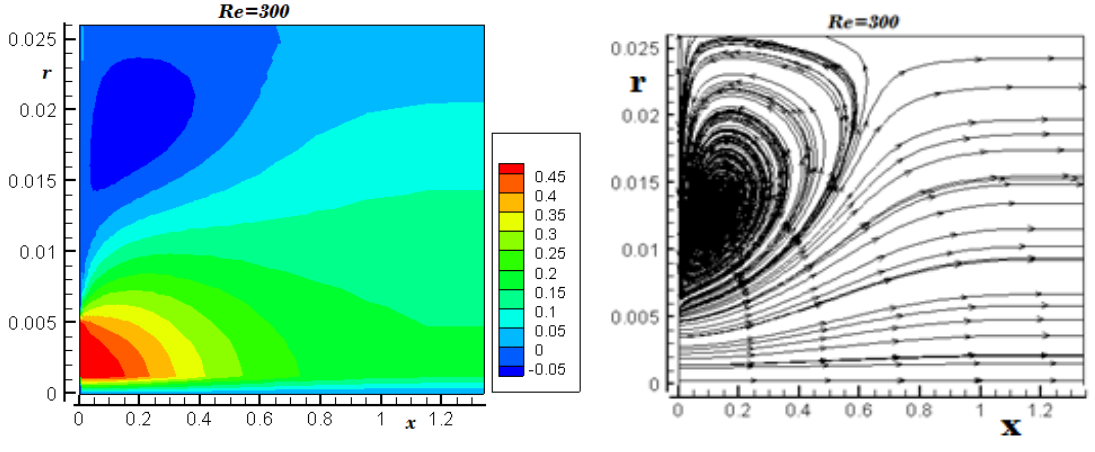

Figure10: Contour plots of velocity U and Streamline in the recirculation zone for Re = 300

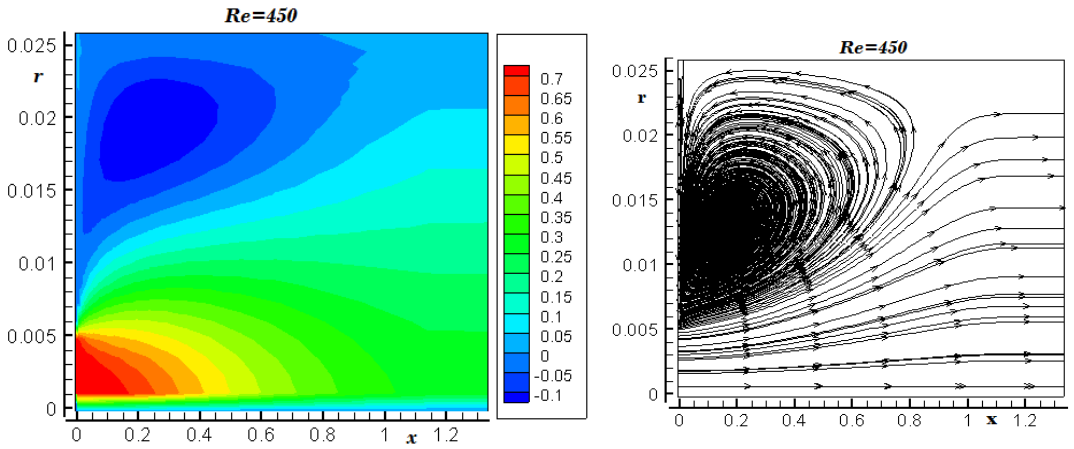

Figure 11: Contour plots of velocity U and Streamline in the recirculation zone for Re = 450

Figure (12) shows the variation of the axial non-dimensional velocity with the non-dimensional radial direction for Re = 100, the magnitude of the axial velocity is maximum at the center of the tube and decreases with increasing the pipe radius r.

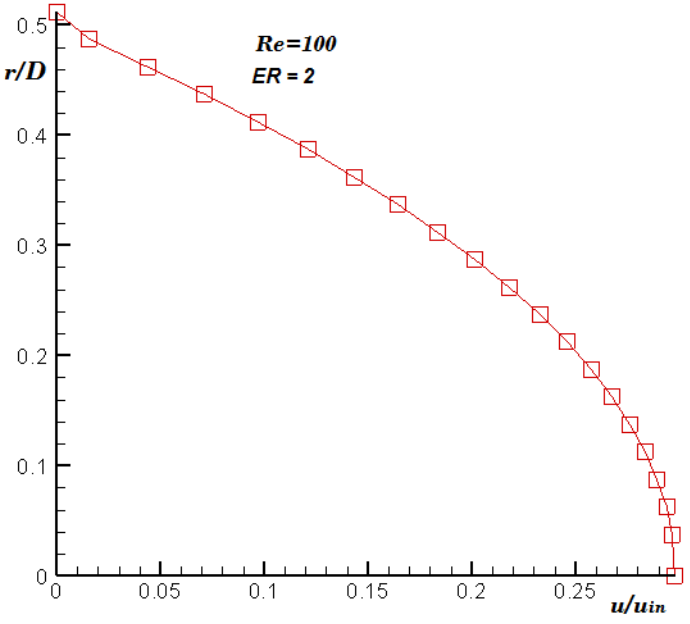

Figure 12: The axial velocity profile.

THE CENTERLINE VELOCITY (U_c):

The centerline velocity profile starts with a value of U_c/U_{in}=1 at the expansion point. The present work predicts that this ratio becomes 0.3 at regions of fully developed flow. It can be seen in Figure (13) that the value of 0.3 is attained within the length given in the domain. Figure (13) gives a comparison of the present results with the results of [7].

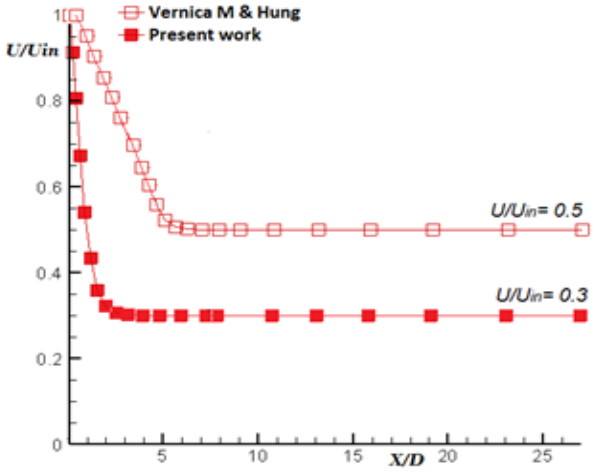

Figure 13: Comparison of the predicted centerline velocity profile at Reynolds number=20.6.

VARIATIONS OF PRESSURE:

It is well known that the pressure is minimum when the velocity is maximum at the expansion point. The pressure is seen to increase with increasing Xr to a maximum value and then decreases slowly to its original value. Figure (14) shows the variation of pressure for Re = 210 and 250. Initially in the post-expansion region, the overall cross-sectional area of the recirculating bubble is high and so the pressure rise is small, further downstream there is more positive pressure. The pressure variation of this work is compared with Ray and Biswas [6] at Re = 223, and Er = 2.

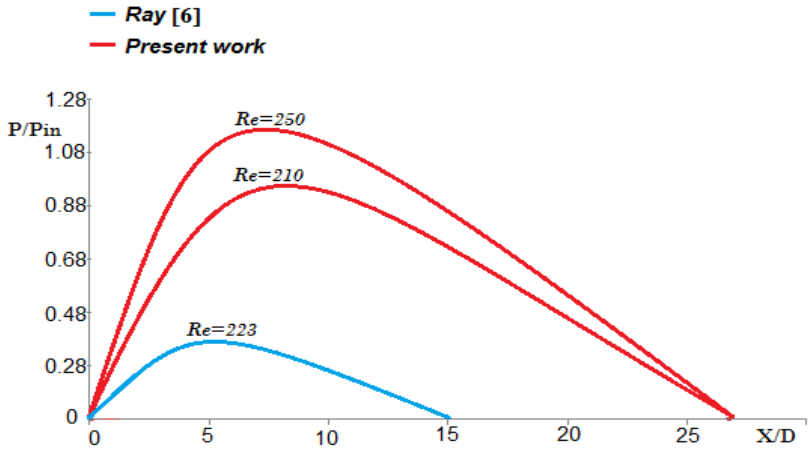

Figure 14: Variations of the pressure on axial distance at different Reynolds numbers.

Figure (15) shows the variation of pressure in x-direction at different values of *r*. It can be seen that the pressure variation with r is very small. The figure reveals that for a low Reynolds number flows maximum pressure occures very close to the expansion point. The peak pressure point is progressively shifted into the direction of the flow (to the right) as the Reynolds number increases; however the pressure recovery is faster for comparatively higher Reynolds numbers**.**

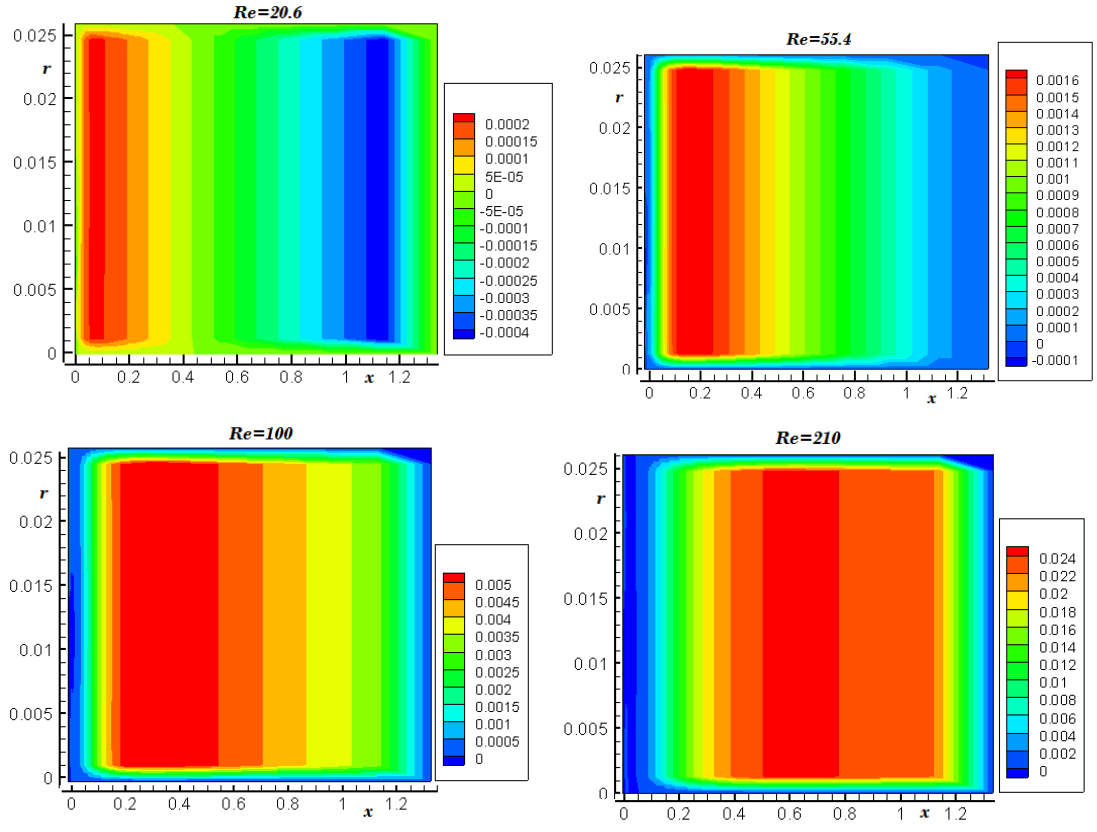

Figure 15: Contour plots of pressure in the sudden expansion for Reynolds number =20.6,55.4, 100 and 210

CONCLUSIONS

The flow characteristics for a low Reynolds number, Re= 20 to 600, and for a fixed expansion ratio, ER=2, was numerically studied. The discretized equations by using the SIMPLE algorithm were solved. The solution of the fully coupled discretized equations was obtained iteratively using the TDMA method. Results of the reattachment length were investigated and compared with similar results from literature. The relationship between the reattachment length and redevelopment length at different Reynolds numbers was investigated.

The investigation showed that the reattachment length and the redevelopment length were linear functions of the Reynolds number. The analysis revealed that the spatial location of velocity disturbances in the flow is influenced by the flow Reynolds number. It is also observed that the pressure increases increasing the distane at which fully developed flow occurs, *Xr*. The pressure is seen to be minimum at the point of the sudden expansion. Any further increase in Reynolds number results in the formation of the asymmetry flow field about the horizontal axis of the tube, and causes a strong adverse pressure gradient that causes the flow to separate at the wall surrounding the expansion point.

The study has provided detailed numerical results for varying the size of the grids and fixed expansion ratio by varying the Reynolds number. The flow domain is covered by a (22x22) mesh system. Any more fine meshes or higher mesh numbers is found unnecessary.

The numerical results of this work are found to be in a good agreement with the experimental work reported by in literature.

REFERENCES

[1] Macagno EO, Hung TK. Computational and Experimental study of a Capative Annular Eddy. J. Fluid Mech 1967; 28: 43-64.

[2] Durst F, Melling A, Whitelaw JH. Low Reynolds Number Flow over a Plane Symmetrical Sudden Expansion. Journal of Fluid Mechanics 1974; 64: 111-128.

[3] Durst F, Pereira JCF, Tropea C. The Plane Symmetric Sudden Expansion Flow at Low Reynolds Numbers. J. Fluid Mech 1993; 248: 567-581.

[4] Oliveira PJ, Pinho FT. Pressure Drop Coefficient of Laminar Newtonian Flow in Axisymmetric Sudden Expansions. Int. J. Heat and Fluid Flow 1997; 18: 518-529.

[5] Hammad KJ, Otugen MV, Arik EB. A PIV study of the Laminar Axisymmetric Sudden Expansion Flow. Experiments in Fluids 1999; 26: 266-272.

[6] Sudipta Ray, Nirmalendu Biswas, Prokash C. Investigation of Newtonian Fluid Flow through a Two-dimensional Sudden Expansion and Sudden Contraction Flow Passage. Roy, Department of Mechanical Engineering, Jadavpur University, Kolkata – 700 032-July2012, India, International Journal of Engineering Research and Development

[7] Vernica M. Carrillo, John E. Petrio. Application of the grid convergence index to a laminar axi-symmetric sudden expansion flow. Albrook Hydraulics Laboratory, Department of Civil and Environmental Engineering, Washington State University, USA,99164-2910-2014.

[8] Li Yinpeng, Wang Changjin, Ha Mingda. Discussion on Local Resistance Coefficient of Sudden Expansion Pipe, Journal of Applied Science and Engineering Innovation Vol.2 No.2 2015

NOMENCLATURE

A	Coefficient of Discretization Equation (a_P , a_W , a_E , a_S , a_N)
b	Mass source Term
D	Diffusion Conductance (D_w, D_e, D_s, D_n).
C	Convective Mass Flux per Unit Area (C_w , C_e , C_s , C_n)

g	Gravitational acceleration [m/s^2]
ρ	Fluid density [kg/m^3]
P	Pressure [N/m^2]
$P*$	Guessed Pressure Field [N/m^2]
P'	Pressure Correction [N/m^2]
P_e	Local Grid Peclet Number
S	Source
u	Velocity in x-Direction [m/s]
u'	Velocity Correction in x-Direction [m/s]
$u*$	Guessed Velocity in x-Direction [m/s]
x, r	Cylindrical Coordinates
μ	Dynamic viscosity[kg/m-s]
ρ_0	Reference density [kg/m^3]
d	small diameter of the pipe [m]
ER	Expansion ratio (D/d)
Xr	Reattachment length [m]
D	Large diameter of the pipe [m]
R_e	Reynolds number = $\frac{\bar{U}\,D}{v}$
v	Kinematic viscosity [μ/ρ]
L_D	*Redevelopment length* [m]
U_c	Reversed velocity [m/s]